Study of the contamination of muons by punch-through of gamma showers in a muon detector.

C. Ghesquière. LPC Collège de France (Paris)
A. Wasilewski, J. Wdowczyk. Inst. of Nuclear Physics (Lodz)

Resumé:

L'expérience THEMISTOCLE prévoyait dans son extension des détecteurs de muons associés aux télescopes Cerenkov, afin de distinguer les gerbes hadroniques des gerbes gammas.

Dans l'hypothèse d'un détecteur composé de couches alternées d'absorbeurs et de compteurs Geiger-Muller, on calcule par Monte-Carlo la probabilité de simulation d'un muon par un gamma (ou électron) pénétrant, en fonction de l'énergie incidente et des épaisseurs d'absorbeur. On en déduit des formules empiriques d'interpolation sur une large bande d'énergie.

A titre d'exemple, le nombre de muons simulés par des gammas associés à des cosmiques de 100 et 1000 TeV est calculé selon diverses hypothèses.

Abstract :

To complement the THEMISTOCLE Cerenkov telescopes, muon detectors were foreseen in order to help discriminate hadronic showers from Electro-magnetic . ones.

Following a scheme of Geiger-Muller counters sandwiched between absorbers (iron or concrete) the number of punch-through gamma showers faking muons is calculated by Monte-Carlo methods, as a function of energy and absorber thickness. From there, empirical formulas are deduced to interpolate between large ranges of energies.

As typical exemples the number of punch-through associated to 100 and 1000 TeV cosmic ray showers are calculated.

Key-words: Cosmic muons, Cosmic ray detection, muon detection

Introduction.

In many cosmic ray Extensive Air Showers (EAS) investigations it appears to be very important to detect muons. This creates the need for designing relatively cheap muon detectors.

The needs for muon detection occur in the case of observing the high energy gamma-rays from point sources and also in the case of observing the very large extensive air showers. In the first case the detection of muons would indicate the existence of certain irregularities in the cross-section for photoproduction in high energy gamma-air nuclei interactions, in the second case the detailed information on the shape of the muon lateral distribution could disclose the nature of the primary particles initiating the showers (in particular the nuclear mass of the particles) as it has been pointed out by Chi et. al (1).

Those authors have fitted the Sydney data on large showers with muon lateral distribution of the form

$$\rho_\mu(r) = A\left(\frac{r}{r_0}\right)^{-0.75}\left(1+\frac{r}{r_0}\right)^{-3.4} \qquad (1)$$

where the r_0 parameter is allowed to vary from shower to shower. The obtained value of the r_0 parameter can be used as the indicator of the height of the shower maximum and that in turn as the indication of the primary particle nuclear mass. The parameter r_0 can be converted into x_m (the pressure or atmospheric depth of the level where the muons are effectively generated) using a simple geometrical formula

$$x_m = \frac{1000}{\cos\Theta_{ZN}}\exp\left(-\frac{r_0\cos\Theta_{ZN}}{400}\right) \qquad \text{All units in m} \qquad (2)$$

In that way there was obtained a parameter x_m characterising the width of the muon lateral distribution in a given shower.That parameter can be used to indicate the nuclear mass of the primary particle. An Important point which should be stressed here is that the main source of the r_0 variation (namely the change of the zenithal angle of the shower arrival direction) is taken out.

The determination of the primary particle masses may disclose some details of high energy cosmic ray particles propagation in the galactic magnetic field and by at the same time may provide information about the structure properties and locations of the cosmic ray sources in particular in our Galaxy.

The design problems for simple muon detector have been discussed in the present paper using as an example the detector suggested for the Themistocle experiment (2). That design has been based on the use of several GM counter layers separated by layers of absorber.

The main drawback of that design is the probability that some muon tracks can be simulated by the punch through of the local showers initiated by relatively high energy photons and electrons which are always present in the showers. The present analysis concentrates on Monte-Carlo simulation of such showers in the absorbers at fixed particle energy.

The drawback of the analysis is that it is limited to the rather particular design for the Themistocle experiment.. It should be however stressed that designing of muons detectors based on the same principle has been envisaged for other experiments; in the case of the KASKADA experiments a muon detector based on a spark chamber layer under their main hadron detector is proposed in order to increase the muon detector power. In the case of the HEGRA experiment in the Canarian Islands, it is proposed to use layers of GM counters under absorbers, like in the Themistocle case. The results of the present analysis can be used in the actual design of those detectors.

Detector description.

The detector is defined by three layers of absorbers sandwiching three layers of detectors (Fig 1)

At the top 2 cm of iron (1.14 X_0) stop the very low energy component of gammas and electrons which will spoil the first layer of detector.

The middle layer is a thick slab of iron at successively 20, 30 and 40 cm thickness (11.4, 17.5,and 23.5 X_0) in the calculations.

The bottom layer consists of successively 100,150 and 200 cm of concrete (9.4, 14.0 and 18.7 X_0) , making the last stage of filtering.

The three layers of detectors are assumed to have a firing threshold of 4 MeV, which is a reasonable limit for the Geiger tubes to be used.

Program.

The program used is a full Monte-Carlo which follows all the tracks down the 4 MeV cut-off. This program KASKADA was written by the Lodz group (Ref 2).

As there are large dispersions and tails in the distributions of particles, a large number of showers have to be generated in order to reach a sufficient degree

of confidence in the determination of the average punch-through. The errors stay anyway very large and not gaussian, hence it is difficult to evaluate confidence levels from the distributions.

For the distributions shown later we shall quote only central values, then keeping in mind that the confidence level is then around 50% .

The procedure followed is such:

1) The punch-through probabilities are estimated for gammas of fixed energies incident on the detector, with enough statistics.

2) Analytic formulas are obtained to interpolate the probabilities over all energies and thicknesses of absorber.

3) The analytic formulas are used to calculate the punch-through in showers of a high energy gamma incident on top of the atmosphere and giving particles with a large spread in energy at the level of the detector.

Probability of punch-through for a single gamma.

The punch-through is defined as at least one particle of energy >4MeV hitting the last plane of detector after all the absorbers.

The punch-through probability is the ratio of showers giving punch-through to the number of gammas incident on the stack.

The calculations were done for the nine combinations of layer thicknesses 2 (20,30 and 40 cm) and 3 (100,150 and 200 cm), for incident energies of 1,10,100 and1000 GeV .

The punch-through probabilities corresponding to the different combinations of absorbers are plotted in fig 2 and 3 as a function of the gamma energy.

Within the uncertainties, which are large on some points, the punch-through probabilities for gammas may be approximated by the formula :

$$P(E_g) = \left(1 - \exp - \left(\frac{E_g}{A(X)}\right)^{1.2}\right)^{1.21} \qquad (3)$$

X being the total thickness of absorbers in rad. length.

The values of A(X) obtained by fitting on Fig 2 and 3 are tabulated in table 1. and plotted in Fig.4

The variation af A as a function of X is smooth enough to be interpolated by an analytic expression which is fitted on Fig 4 and gives the formula:

$$A(X) = 35 \exp\left(0.246 (X - 20)\right) \qquad (4)$$

Those two formulas (3) and (4) allow to interpolate over a wide range of energies and absorbers and will be applied for the punch-through of atmospheric showers.

Punch-through of showers.

Showers of 100 and 1000 TeV are Monte Carlo simulated and the distribution of gammas as a function of their energy and their distance to the shower axis are obtained. Those distributions are shown in scatter plots Fig 5 and 6.

Then the punch-through probability is applied on each gamma and the scatter plots Fig 7 to 12 display the number of gammas associated to a 1000 TeV primary shower having given a punch-through according to their initial energy and their radial distance r.

At 100 TeV, only the plot corresponding to the thinnest absorber is shown, (Fig 13), all others being empty.

The total probability of punch-through is calculated by summing over all individual punch-through irrespective of the energies and distances. However there may be different way to characterise it :

1) Global probability that at least one particle of the shower leaks from the absorber. It correspond to table 2 line 1.

2) Global probabbility that at least one particle leaks outside of a circle of 100 cm centered on the axis. Table 2 line 2.

3) Average number of particles leaking from absorber per shower. Table 2, line3.

4) Average number of particles leaking outside of a radius of 100 cm. Table 2, line 4.

The first and second lines are useful to help for the choice of the set-up, the last ones, to correct the observed number of muons by subtracting the punch-through on a statistical basis.

Remarks.

It appears that from the point of view of the punch-through, only the last detector layer is useful. Nevertheless without knowing the shower axis with a small enough uncertainty, it is difficult to apply the criteria of core elimination where the contamination will eventually be high.

To avoid this problem and at the same time to obtain a confirmation of a real muon track, it seems mandatory to use a second detector plane at the intermediate

position between the two thick absorbers. This detector will provide two informations:

1) Keep track of the muon and confirm it by coincidence, giving also information about the direction.

2) Give through the particles leaking from the second layer of absorber an image of the core position, saturated with particles but still providing a position with an accuracy << 100 cm.

The first detector layer and consequently the first absorber do not appear necessary if one does not want further informations about the muons, for instance the initial direction or a measurement of the multiple scattering angle when crossing the absorbers.

Conclusions.

The calculated punch-through probabilities are only function of X. The simulation of showers so far have only been done for our experimental altitude (1650 m) and for vertical shower; the distribution of particles will change according to the zenith angle, so a more complete study will be necessary. Nevertheless one can already conclude that if one does want to be on the safe side for the quality of the muon signal and keep as much as possible of the muons close of the axis, a minimun thickness of absorber is required: 40 cm of iron and 100 of concrete, or rather, equivalently, 30 cm of iron and 150 of concrete. Then cutting at 1 m of the axis the contamination turns to be negligible at 1000 TeV.

For showers away from the zenith the air absorption is bigger and it is more favorable to kill the punch-through but then edge effects from the boundaries of the detectors appear and make the problem strongly dependent on the detailed set-up.

A good analysis will request at least two layers of absorber and two of detectors. The first detector placed at some 14 Xo depth still provides a good precision on the core position, which may be a big help to the reconstruction of the Cerenkov image as well as to the signature of the muon.

Acknowledgments.

This paper is the result of the collaboration between members of the two institutes made possible through the Collaboration between IN2P3 and the polish laboratories; one of us particularly acknowledges the possibility to use the computer facilities of the CCIN2P3 during his stay in France.

References.

[1] Chi X., Wdowczyk J., Wolfendale A.W.,
J. of Phys. G:1992 in Press

[2] THEMISTOCLE: a high angular resolution Cerenkov light detector.
F. Kovacs. N. Ph. B 14 A (1990) 330

[3] KASKADA; A program developped by E. Krys.and A. Wasilewski
Private communication .....

Table captions.

Table 1: Values of A(x) for different combinations of the absorbers between the detector levels.

Table 2: The punch-through probabilities and average number of electromagnetic showers for a cosmic ray of fixed energy(1000 TeV) as a function of the absorber thickness and distance to shower axis.

Figure captions.

Fig 1 : Scheme of absorber and detector lay-out.

Fig 2 Probability of punch-through as a function of gamma energy for several combinations of absorbers :

1) 2 - 20 - 100 cm (Pa)
2) 2 - 30 - 100 cm (Pb)
3) 2 - 40 - 100 cm (Pc)

Fig 3 : Same as fig 2 for absorbers :

4) 2 - 20 - 150 cm (Ne a)
5) 2 - 30 - 150 cm (Ne b)
6) 2 - 40 - 150 cm (Ne c)

Fig 4 : Values of A as a function of X = Number of Rad. Length.

Fig 5 : $dn / dE_g\, dr$ at the detector level for a 1000 TeV vertical shower in atmosphere .

Fig 6 : $dn / dE_g\, dr$ at the detector level for a 100 Tev vertical shower in Atmosphere.

Fig. 7: $dn_{\text{punch-through}} / dE_g\, dr$: Number of gammas giving a punch-through in the third layer of detector for a 1000 TeV gamma at zenith in atmosphere, for absorber 2 - 20 - 100 cm

Fig 8 : Same as 7 for absorber 2 - 30 - 100 cm

Fig 9 : " 2 - 40 - 100 cm

Fig 10: " 2 - 20 - 150 cm

Fig 11: " 2 - 30 - 150 cm

Fig 12: " 2 - 40 - 150 cm

Fig 13: $dn_{\text{punch-through}} / dE_g\, dr$: Number of gamma giving a punch_through in the third layer of absorber for a 100 TeV gamma at zenith in atmosphere, for absorber 2 - 20 - 100 cm.

Table 1

#	Absorbers	X	A (X)
1	2/20/100	22	43
2	2/30/100	28	160
3	2/40/100	34	700
4	2/20/150	26.5	155
5	2/30/150	32.6	600
6	2/40/150	38.6	1800
7	2/20/200	31.2	500
8	2/30/200	37.3	1350
9	2/40/200	43.3	2600

Table 2

Absorbers	20/100	30/100	40/100	20/150	30/150	40/150	20/200
P all r	1	1	1	1	1	0.5	0
P r >1m	1	1	0.25	1	0.25	0.25	0
<N> all r	208	41	5	42	6	0.75	0
<N> r>1m	18	3	0.25	4	0.25	0.25	0

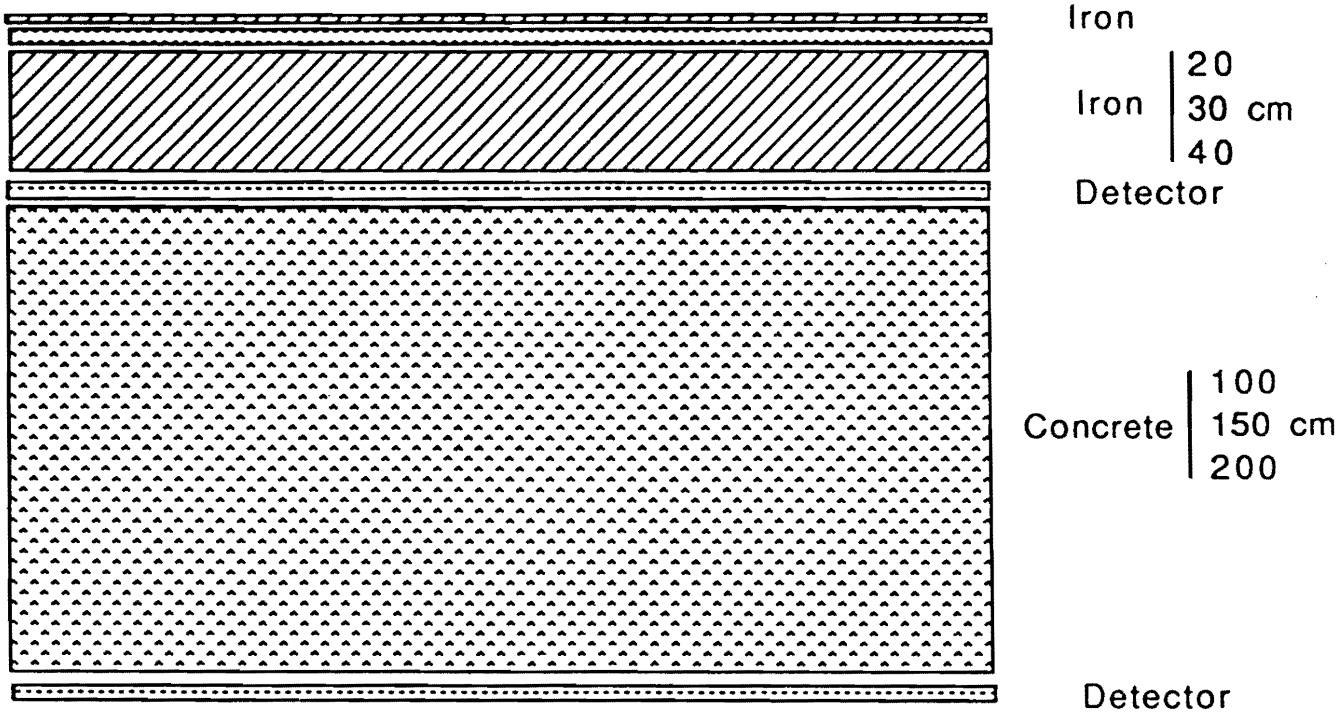
Iron
Iron
20
30 cm
40
Detector
Concrete
100
150 cm
200
Detector

Fig 1

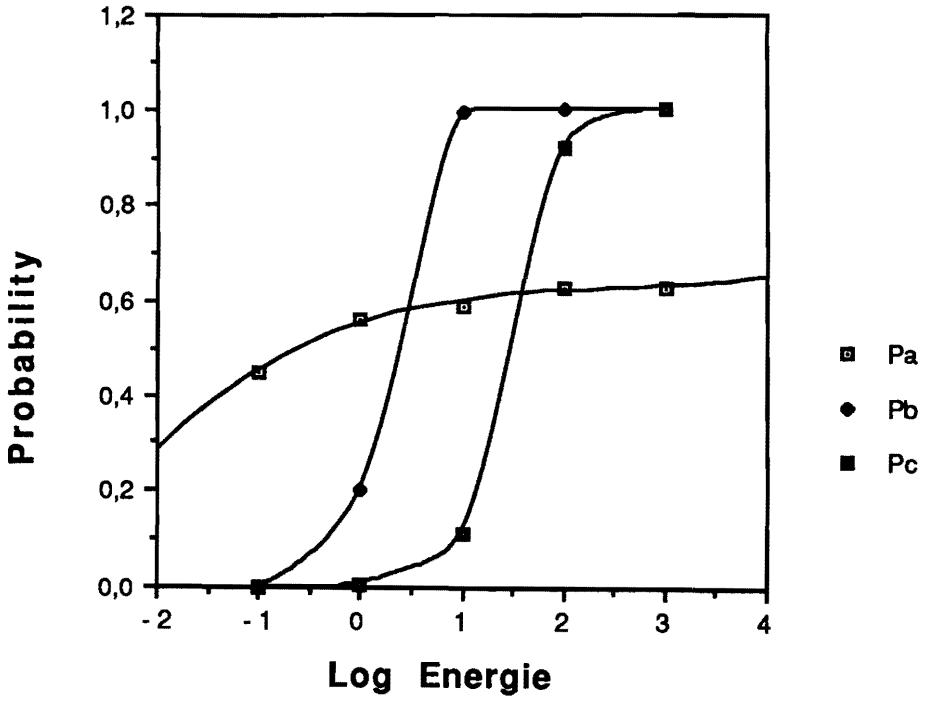

Fig 2

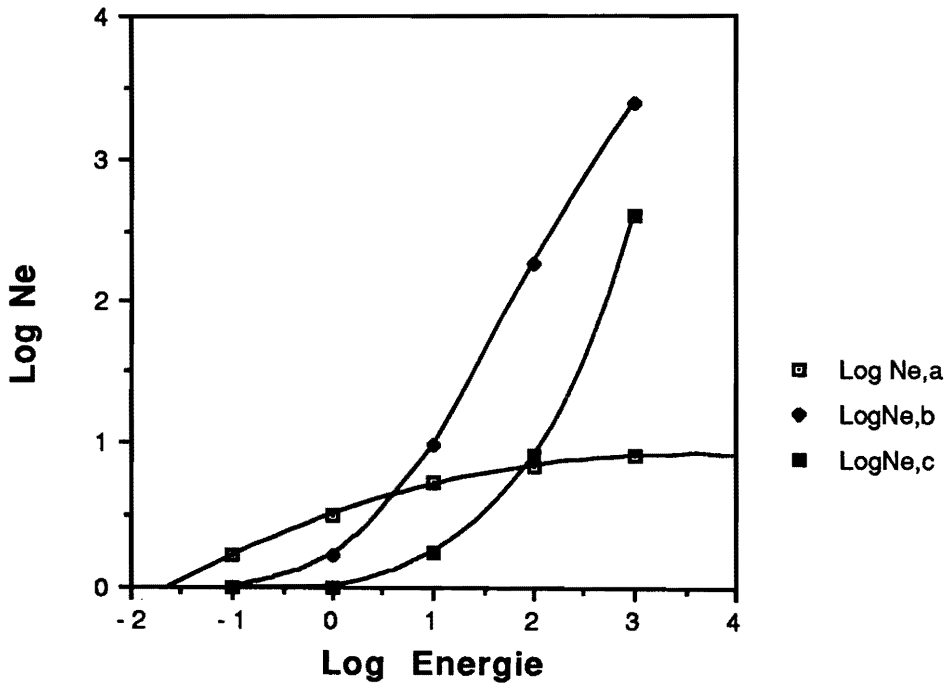

Fig 3

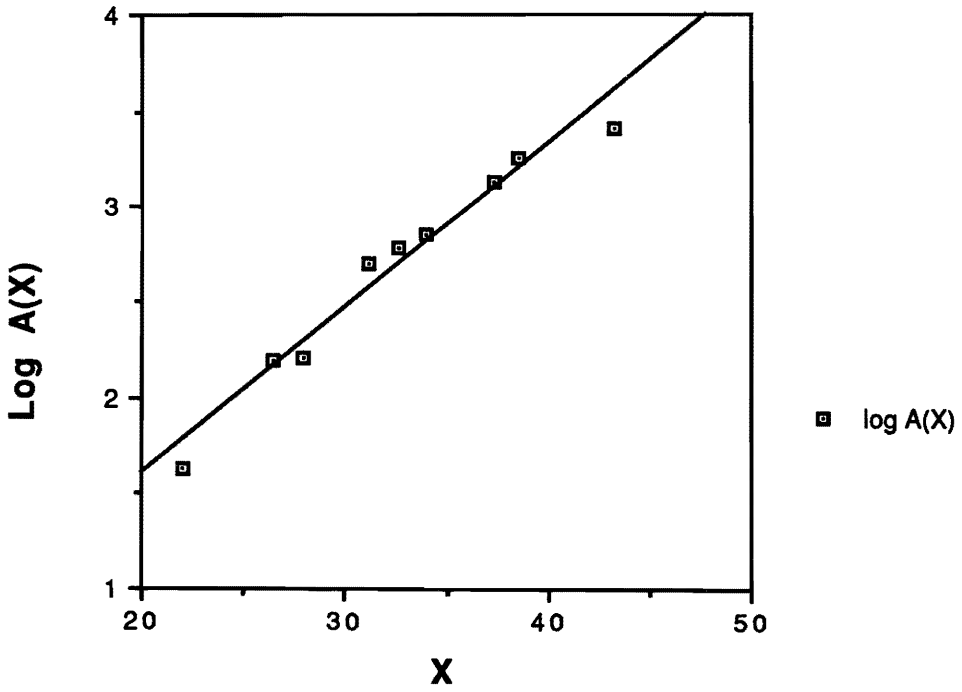

Fig 4

$E_0 = 1000$ TeV

E_γ(GeV)

	0.25														
	0	0													
10^3	0	0.25	0.25												
	0.25	0	0	0	0.5	0.25									
	0	0.5	0.25	0.25	0.25	0									
	0.25	0.25	0.25	0.5	0.25	0.5	0.25	0.25							
	0.25	0.5	0.5	0.75	1.5	1.25	0.5	0.5							
10^2	1	1	1	2	3	2.5	3	1	1	1	0.25				
	2	0.5	1	4	4	4	7.5	9	6.5		5.5		1	1	
	1	2	3	4	7	9	12	19	16	15	6.5	2.5	1	0.25	
	0.5	1	3	3.5	8.5	18	21	30.5	35	29	20	14	4	1	
	3	2.5	4.5	6.5	12	22	36	55.5	73.5	68	59	43	18	9	2	0.5
10															
	1					10					10^2				

Log r (cm)

Fig. 5

$E_0 = 100$ TeV

E_γ (GeV)

10^2	0	0	0	0.15	0.3	0.5	0.3	0	0	0.15					
	0.15	0	0	0.5	0	0.15	0.15	0.15	0.7	0	0	0	0.15		
	0.15	0	0.3	0.5	0.15	0.15	0.5	0.15	1	0.7	0.3	0	0.15		
	0	0	0.3	0.3	0.15	0.5	0.7	0.85	1	0.3	1.3	0.3	0	0.15	
	0.3	0	0.3	0.85	0.5	0.7	0.7	1.7	1.7	2	1.85	1.3	0.7	0.15	0.15
10															
	1					10					10^2				

log r (cm)

Fig 6

$E_0 = 1000$ TeV

E_γ(GeV)

Absorbers : 2/20/100

	0.25														
	0	0													
10^3	0	0.25	0.25												
	0.25	0	0	0	0.5	0.25									
	0	0.5	0.25	0.25	0.25	0									
	0.25	0.25	0.25	0.5	0.25	0.5	0.25	0.25							
	0.25	0.5	0.5	0.75	1.5	1.25	0.5	0.5							
10^2	1	0.75	0.5	1.75	2.5	2.	2	0.75	0.5	1	0.25				
	1	0.25	1	3.25	3.25	2.25	4.5	4.5	4.5	3.5	0.75	0.5	0	0.25	
	0.25	0.75	1.25	1.25	3.75	4	6.5	8.5	7.5	7	2	1.25	0.25	0.25	
	0.25	0.5	0.75	0.5	2	5	5.5	7	8	6.5	7	5	1	0	
	0.25	0	0	0.75	4.25	4.25	6	8.5	11	11	7	6.5	2.5	0.75	0 0
10															
	1					10						10^2			

Fig. 7

E_γ (GeV)

Absorbers 2/30/100

	0.25													
	0	0												
10^3	0	0.25	0.25											
	0.25	0	0	0	0.5	0.25								
	0	0.25	0.25	0.25	0.25	0								
	0	0.25	0.25	0	0.25	0.25								
	0.25	0.25	0.25	0.25	0.75	0.5	0.5	0.25						
10^2	0.25	0.25	0	0.75	1	0.25	1	0.25						
	0.25	0	0.25	1	0.5	0.25	1.25	1.5	0.75	0.5	0.25	0.25	0	0.25
	0	0.25	0.25	0	0.25	0.75	1	0.75	1	1.5	0.5	0.25	0	0
	0.25	0	0	0.25	0.5	1	1.25	0.5	2	1.5	1.75	1	0	0
	0	0	0	0	0.25	0.25	1.75	1.5	0.75	1.5	0.75	0.75	0.25	0.25
10														
	1					10						10^2		

Fig 8

E_γ (GeV)

Absorbers : 2/40/100

	0.25											
	0	0										
10^3	0	0.25	0.25									
	0	0	0									
	0	0	0	0.25	0.25							
	0	0	0	0	0.25							
	0	0	0.25	0	0.25							
10^2	0	0	0	0	0.25							
	0	0	0	0	0.25	0	0	0.25	0	0	0.25	
	0	0	0	0	0	0	0	0	0	0	0.25	
	0	0	0	0	0	0	0	0	0.5	0	0.5	
	0	0	0	0	0	0	0.25	0	0	0.25	0	0.25
10												
	1					10					10^2	

log r (cm)

Fig 9

$E_0 = 1000$ TeV

E_γ(GeV)

Absorbers : 2/20/150

	0.25														
	0	0													
10^3	0	0.25	0.25												
	0.25	0	0	0	0.5	0.25									
	0	0.25	0.25	0.25	0.25	0									
	0	0.25	0.25	0	0.25	0.25	0	0							
	0.25	0.25	0.25	0.25	0.75	0.5	0.5	0.25							
10^2	0.25	0.25	0	0.75	1	0.5	1	0.25	0	0.25	0				
	0.25	0	0.25	1	0.5	025	1.25	15	0.75	0.5	0.25	0.25	0	0.25	
	0	0.25	025	0	0.25	0.75	1	1	1.25	1.75	0.5	025	0	0	
	0.25	0	0	0.25	0.5	0.5	1.25	0.5	2	1.5	1.75	1	0	0	
	0	0	0	0	0.25	0.25	0.75	15	0.75	1.5	0.75	1.5	0.75	0.25	0.25
10															
	1					10						10^2			

Fig. 10

E_γ (GeV)

Absorbers 2/30/150

	0.25											
	0	0										
10^3	0	0.25	0.25									
	0	0	0									
	0	0.25	0.25									
	0	0	0	0	0.25							
	0	0	0.25	0	0.25							
10^2	0	0	0	0	0.25	0	0.25					
	0	0	0	0.25	0.25	0	0.5	0	0	0.25		
	0	0	0	0	0	0	0	0	0	0	0.25	
	0.25	0	0	0	0	0	0	0	0.5	0	0.5	
	0	0	0	0	0	0	0.25	0	0	0.25	0	0.25
10												
	1					10						10^2

Fig 11

E_γ (GeV)

Absorbers : 2/40/150

	0.25											
	0	0										
10^3	0	0										
	0	0										
	0	0										
	0	0										
	0	0										
10^2	0	0										
	0	0										
	0	0										
	0	0										
	0	0	0	0	0	0	0.25	0	0	0	0	0.25
10												
	1					10						10^2

log r (cm)

Fig 12

$E_0 = 100$ TeV

E_γ (GeV)

Absorbers 2/20/100

10^2	0	0	0	0.15.	0.3	0.5	0.15	0	0	0.15		
	0	0	0.	0.5	0	0	0.15	0	0.15	0		
	0	0	0	0.15	0	0	0.3	0.15	0.7	0.5	0.3	
	0.	0	0	0.15	0	0.3	0.15	0	0.15	0.3	0.5	0.15
10	0	0	0	0.3	0	0.5	0.15	0.15	0.5	0.15	0.5	0.15
	1					10					10^2	

Fig 13